# Modeling of Confined Inflatable Structures

Eduardo M. Sosa[*], Choo-Siang Wong[†] and Ever J. Barbero[†]

[*]Department of Civil and Environmental Engineering
West Virginia University, Morgantown, WV, USA

[†]Department of Mechanical and Aerospace Engineering
West Virginia University, Morgantown, WV, USA

***Abstract***: *This work presents the development of Finite Element (FE) models to simulate different stages of the design and operation of constrained inflatable structures. Such structures can be used, for example, for sealing segments of underground civil infrastructure such as large pipes or tunnels. In such applications, the confined inflatable structure is prepared for placement, either permanently or temporally, and left ready for deployment, inflation, and pressurization when needed. Once positioned and in operation, the inflatable may be subject to a number of possible loading scenarios and interaction with the surrounding confining environment, which must be evaluated beforehand. FE models developed for this work include models for folding, positioning, deployment, pressurization, and in-service loading of constrained inflatable structures. Models were created and analyzed with the Simulia/Abaqus simulation suite. Membrane materials, relaxation techniques, mass scaling, as well as a multi-chamber approach were evaluated and implemented in order to better correlate predicted results to available experimental data. The result is a modeling procedure that can be used to predict the performance of an inflatable structure for a given confining environment. Thus, the models can be used as a predicting tool for optimization of different aspects of the design and field operation of the inflatable structure.*

***Keywords***: *Abaqus/CAE, Abaqus/Explicit, Confined Inflatable, Deployment, Folding, Membrane.*

## 1. Introduction

Large inflatable structures for protection of underground infrastructure, such as railway tunnels or large pipes, has been under development at West Virginia University (WVU) since 2007 (Barrie, 2008, Martinez et al, 2012, Fountain, 2012, Barbero et al, 2013-a/b and Sosa et al, 2014-a/b). The implementation of large inflatable structures (also called inflatable plugs) inside civil infrastructure such as transportation tunnels is intended to prevent or reduce the damage induced by hazardous events by creating a compartment to contain the threat. Potential threats include flooding, smoke or noxious gases that can propagate along a tunnel system and compromise its functionality and structural integrity. The inflatable structures are typically installed at specific locations of the tunnel in order to create a compartment that can isolate the compromised region. As part of this development, WVU has designed several prototypes (Barbero et al, 2013-b) and conducted multiple validation tests of confined inflatable structures at full and reduced scale (Martinez et al, 2012, Barbero et al, 2013-a, Sosa et al, 2014-a/b). Some of these validation tests were performed using specially built testing facilities designed to simulate a segment of an actual rail transportation tunnel (Barbero et al, 2013-a, Sosa et al, 2014-a/b).

However, performing tests, especially at full-scale in either an actual tunnel segment, or in the specially built testing facilities, is a very complex task. Validation tests performed at full-scale demonstrated that it can take several iterations to achieve acceptable results which cannot be predicted in advance. Therefore, the development of numerical models using Finite Element Analysis (FEA) becomes imperative as a predicting tool that can anticipate the change in performance of the system under design and operational changes. Calibrated models are also used for parametric studies and design optimization that otherwise would be very costly to implement at experimental level. Examples of tests performed at full-scale are illustrated in Figure 1. Additional details on testing configurations and experimental results are reported by Martinez et al, 2012, Barbero et al, 2013-a, Peil et al, 2012 and Sosa et al, 2014-a/b.


**Figure 1: Full-Scale Inflatable Plugs: a) Test performed in an actual tunnel in 2008 (Barrie, 2008, Martinez et al, 2012); b) and c) Tests performed at WVU (Barbero et al, 2013-a, Sosa et al, 2014-a/b).**

This paper aims to introduce some of the work carried out for the development of FE models of confined inflatable structures used for protection of underground tunnels. These models were created and analyzed based on information available from experimental results of tests performed at full-scale (Barbero et al, 2013-a; Sosa et al, 2014-a/b). The two main objectives of this study are:

1. Development of FE models of confined inflatable plugs to simulate:
    a. The structural components of the inflatable
    b. The folding process of the inflatable
    c. The deployment of the inflatable under confined conditions
    d. The interaction of the inflatable with different elements of the confining surface and the global and local conformity to those elements
2. Comparison of numerical results with available experimental data in order to adjust modeling parameters and improve the predicting capability of the models.

# 2. Finite Element Model Setup

## 2.1 Modeling Tools

Abaqus/CAE and Altair's HyperMesh were chosen as finite element pre-processors for creating geometries, meshing and renumbering of nodes and elements into a scripting-friendly form. For solving the models, Abaqus/Standard and Abaqus/Explicit were selected to solve the simulations. In the post-processing phase, Python, Tool Command Language (TCL) Script, and Abaqus Scripting were implemented to generate numerical outputs, and Abaqus/CAE was used to visualize and present the numerical results graphically.

## 2.2 Geometries

The development of a comprehensive model able to reproduce the different stages of the work performed experimentally required the creation of several components that constituted the whole model. The two main components are the inflatable plug and the confining environment representative of a typical tunnel segment in which the inflatable will be installed. Additional components used in the modeling process included auxiliary planes representative of sitting base and tools and procedures that were used during the folding process of an actual full-scale prototype. The features of the different components of the FE model were created considering the different stages of implementation of an inflatable structure in a tunnel section. These stages included folding, placement in the storage area, relaxation, and deployment of the inflatable plug.

The first main component of the FE model is the inflatable plug. It consists of a cylinder with two hemispherical end-caps. Each hemispherical end-cap includes three partitions on its surface created for manufacturing purposes as illustrated in Figure 2. The perimeter of the cylindrical portion of the inflatable is designed to be larger than tunnel's perimeter. Over sizing is added to achieve conformance of the plug to the enclosure taking into account wrinkles and sag that may occur during deployment. Better fitting, or conformance, result in better sealing, which is the ultimate objective of the system.

The structural membrane of the inflatable consist of a multiple layer system. The multi-layer system is modeled with an equivalent single membrane built from M3D4 membrane elements with equivalent thickness, mass and stiffness representative of the macro-mechanical behavior of the structural membrane. The inflatable plug also includes two metal fittings used as air fill and air release ports. These two fitting are located on one of the hemispherical end-caps. Since they are much more rigid than the structural membrane, they are modeled by R3D4 rigid elements. The total mass of the inflatable plug including metallic fittings is approximately 907 kg.

Figure 2(a) shows how the geometry of the inflatable plug was initially partitioned into several auxiliary surfaces and edges. The purpose of creating these auxiliary surfaces and edges is to delimit the position of fitting areas, internal chamber surfaces, folding surfaces and folding lines at the cylindrical region of the plug. Figure 2(b) shows the meshed configuration of the inflatable plug.

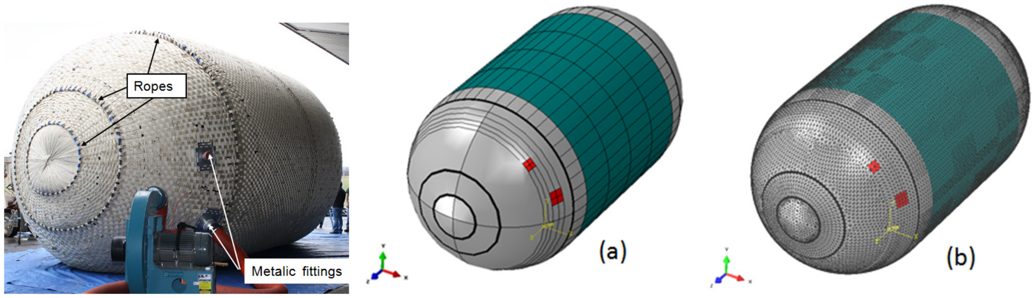


**Figure 2: Inflatable plug: An actual full-scale prototype (left); (a) Initial geometry with auxiliary partitions; (b) Final meshed configuration.**

The second main component of the FE model is the model of the tunnel section. In this study, the tunnel section in which the inflatable plug will be placed is assumed to be non-deformable. A typical tunnel profile is illustrated in Figure 3. This cross section was used for the analyses performed in this work. Figure 3 also shows the 3D geometry and the meshed configuration of the tunnel used for all the analyses. Rigid elements R3D4 were used to represent the tunnel section.

During the folding process, the inflatable plug will interact with a flat base and auxiliary rotational plates created to simulate the folding process. Similarly to the tunnel section, these surfaces are considered non-deformable and were meshed with R3D4 rigid elements. Figure 4 displays all the components involved in the development of the FE model including the inflatable plug, tunnel, auxiliary base, and auxiliary rotational plates.

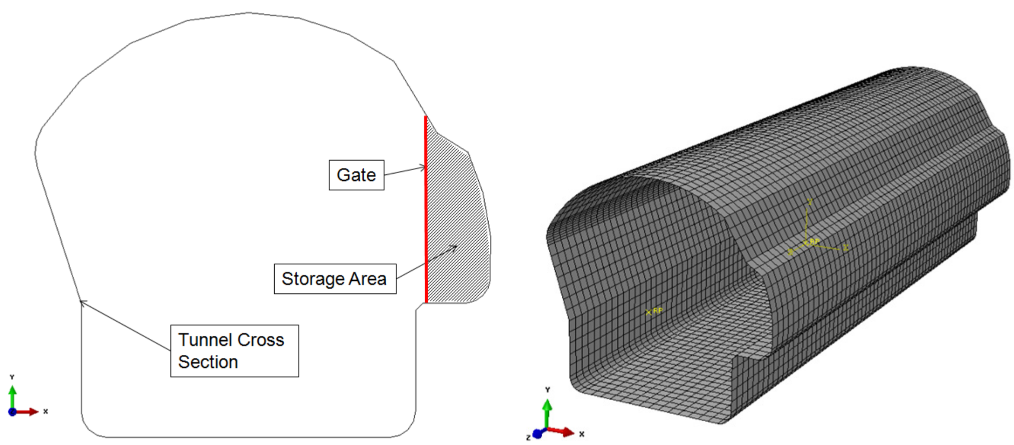


**Figure 3: Tunnel cross section: Typical profile prepared for receiving an inflatable plug (left); Meshed configuration used in the FE models (right).**

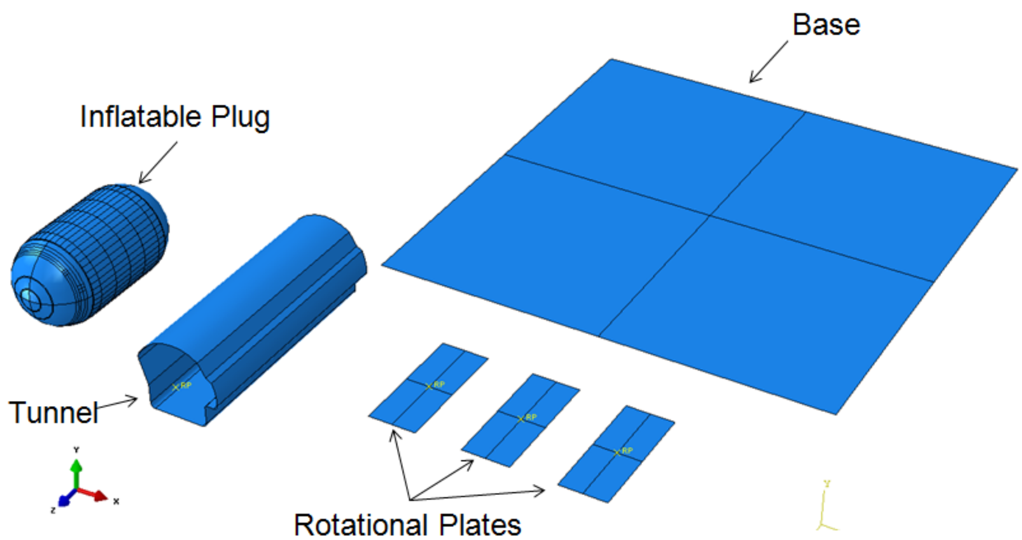


**Figure 4: All components of the FE model.**

## 3. Folding Process

The folding process implemented in this work consisted of a combination of rigid body rotations and translations applied as boundary conditions to selected nodes and elements previously marked on the surface of the inflatable. Folding lines were created from sets of nodes positioned on the surface of the cylindrical portion of the inflatable plug which guided the folding process. The FE model of the folding process is developed as a set of geometric transformations that simulates an actual folding sequence (Barbero et al, 2013-a; Sosa et al, 2014-a).

The model created for simulation of the full folding process included the following general steps: 1) Unconstrained, unstressed inflation; 2) flattening and grounding; 3) and folding by rolling. In the first step, the starting position of the inflatable was in unconstrained and unstressed conditions and using the ideal design geometry. During the second step, the flattening was achieved by simultaneous use of horizontal displacements and vertical gravity force. An illustration of the implementation of these two steps is shown in Figure 5. Once the inflatable is flattened and laying on the ground (represented by the base plate shown in Figure 4), the folding process began by forming a longitudinal wrinkle designed to hold and sequentially release membrane material during the deployment process. This membrane material was held by ties that were modeled by connectors placed discretely along one of the longitudinal edges of the artificial wrinkle. The flattened inflatable at the beginning of the folding sequence is illustrated in Figure 6. The third step of the folding consisted of gradual rolling of the flattened inflatable by successive lifting and partial rotations of the partial folds by using the rotational rigid plates illustrated in Figure 4. Three sets of lifting and rotation maneuvers, combined with gravity force, were applied to complete the folding sequence. Figure 7 illustrates the sequence of the last set of folding maneuvers and the final folded configuration.

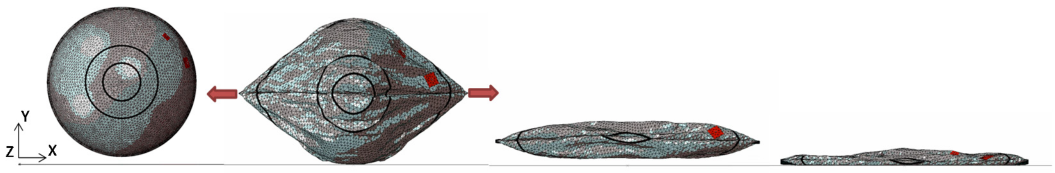


**Figure 5: Sequence of deflation, flattening and grounding in preparation for folding.**

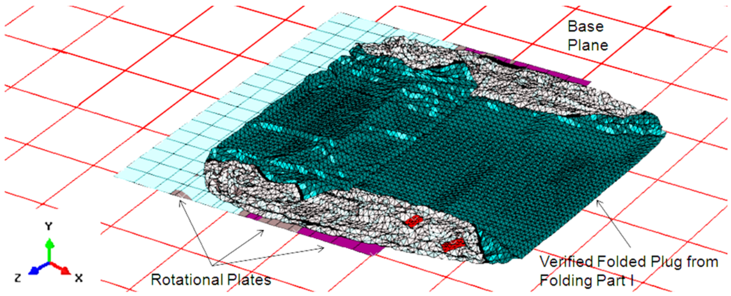


**Figure 6: Flattened inflatable structure at the start of the folding process.**

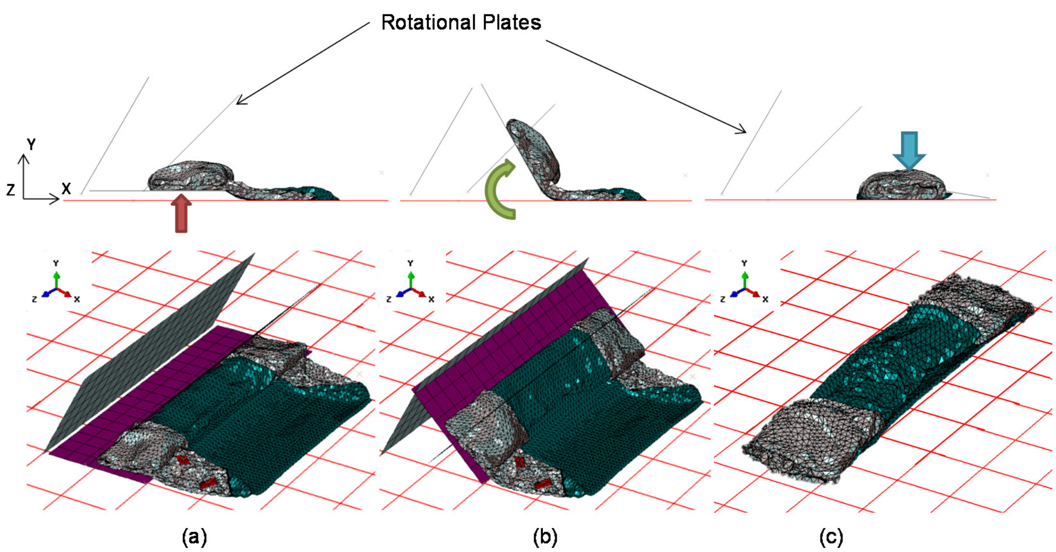


**Figure 7: Folding sequence: (a) Vertical lifting; (b) Rotation; (c) Action of vertical gravity force. This sequence was repeated three times.**

## 4. Positioning of the folded inflatable

The simulation of the placement process consists of a combination of a rigid body rotations and translations of the folded plug in order to place it in the storage area. Once in place, the folded plug is connected to the tunnel along a predefined horizontal line located inside the storage area that provides alignment to the inflatable during the deployment and inflation process. The placement is completed by further translation originated by a horizontal gravity force. Figure 8 shows different views of the placement sequence of the folded plug within the tunnel section. Once the folded plug is positioned in the storage area, a vertical rigid plane that represents an actual enclosure holds the folded plug within the volume available for storage in a typical tunnel section.

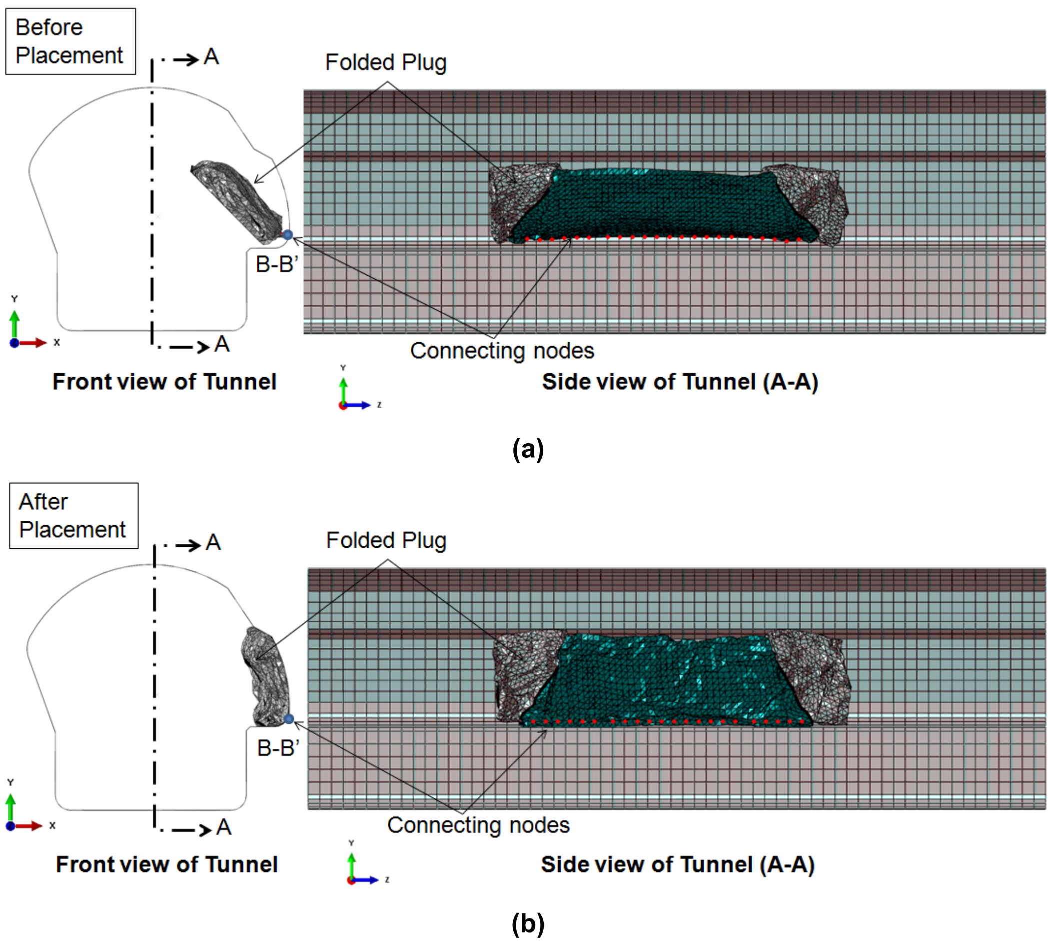


**Figure 8: (a) Initial condition for placement; (b) Orientation of folded plug after rotation and horizontal translation.**

The rigid plane not only simulates the enclosure but also maintains the folded inflatable plug within the storage area during the implementation of the dynamic relaxation process. The main purpose of implementing the dynamic relaxation process into the simulation is to restore distorted elements back to their original condition before doing the deployment simulation. Most of available commercial software execute the relaxation process through passing either node's or element's coordinates from an initial configuration to a reference configuration. In the simulation, the rigid plane pushes and closes the storage area when relaxation simulation commences as illustrated in Figure 9. Figure 9(d) shows the final result of the implementation of dynamic relaxation and gravity force. The result of both effects defined the starting position of the folded plug for the simulation of deployment. The relaxation process is also added to the deployment simulation in order to minimize the kinetic energy, stabilize the simulation process, and avoid distortions on the membrane surface when the inflatable is fully positioned inside the tunnel section.

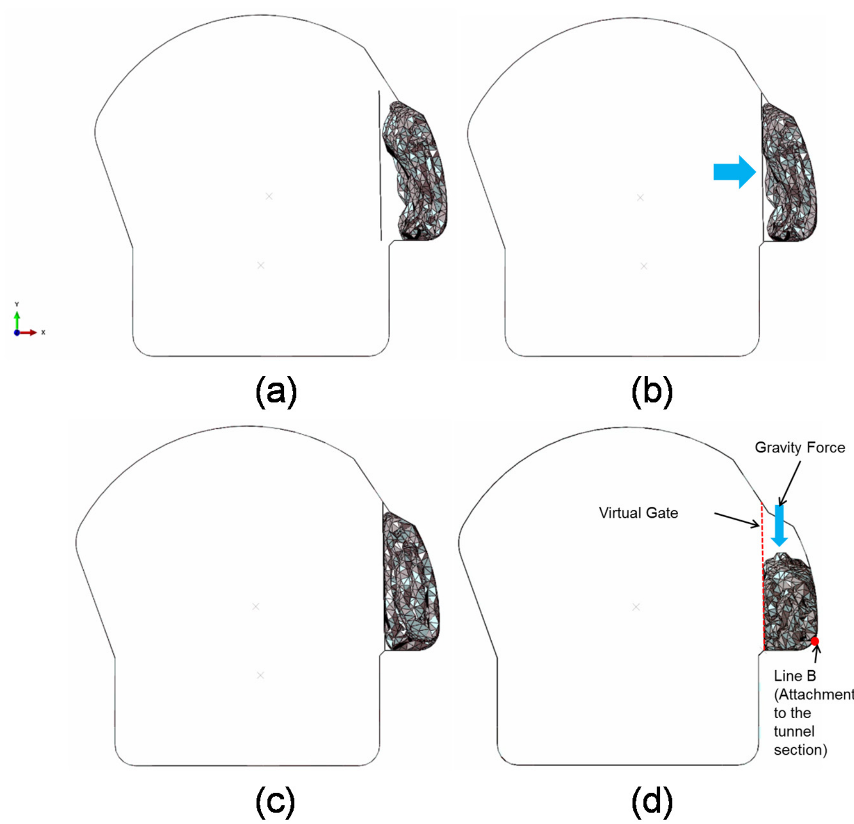


**Figure 9: (a) Rigid plane before closing the storage area; (b) closing the storage area; (c) Folded plug after implementation of dynamic relaxation; (d) Action of vertical gravity force and initial state of the folded plug before deployment.**

# 5. Simulation of Deployment

## 5.1 Inflation Algorithm and Model Setup

The Uniform Pressure Method (UPM) was implemented in this work. This method has been widely used in airbag simulations for more than two decades and demonstrated to predict reasonably good results. The UPM method was found to be simple, computationally efficient and adequate for modeling relatively slow inflation since the inertia of the inflation gas can be neglected. The capability of reproducing the actual deployment behavior with relatively low computational cost and high accuracy were two of the key factors that led to the adoption of the UPM as inflation method. The implementation of more sophisticated algorithms, such as the Coupled Eulerian Lagrangian (CEL) method and the Arbitrary Lagrangian Eulerian (ALE), or mesh-free methods, such as the Smoothed Particle Hydrodynamics (SPH) or the Finite Pointset Method (FPM), was ruled out at this stage primarily because of their elevated computational cost (in the order of about 4 to 15 times higher than UPM depending on the mesh density) and the difficulty of obtaining all the necessary parameters to create an accurate model.

The main assumptions of UPM are that the pressure in the airbag is spatially uniform during the inflation; it also assumes no heat transfer and that the inflating gas behaves as an ideal gas with constant specific heats. A limitation of this simplified algorithm is the inability to simulate local fluid effects because the formulation does not involve the equations of fluid dynamics that describe the movement of fluid. The multi-chamber and the fluid exchange approaches were needed to extend the capability of the UPM in order to replicate the actual deployment behavior obtained from experiments at full-scale.

The UPM is implemented in Abaqus/Explicit based on the formulation proposed by Wang and Nefske (1988). It requires the definition of surface-based cavities to model the fluid-structure interaction during the deployment and inflation process. This capability allows to use standard finite elements to model the membrane of the inflatable; it requires a surface definition on the cavity boundary for coupling the deformation of the membrane and the pressure exerted by the inflation fluid (air in this case); it also requires definition of the fluid behavior, fluid exchange to model the flow of the fluid, and the definition of the inflator properties for modeling the deployment of the cavities. Some of the advantages of implementing a deployment model based on surface-based cavities include the possibility of straightforward modeling of the adiabatic process, a more precise modeling of the inflation process including properties of the multiple cavities (or chambers), as well as relatively rapid convergence of the analysis which shortens the computational time.

Most of the pre-simulation conditions for modeling deployment of a confined inflatable are similar to the ones that are typically applied to simulations of airbags. However, additional assumptions have been made in order to define some of the particular conditions of the simulation. These additional assumptions were based on the behavior observed during actual deployments of full-scale experimental prototypes reported by Barbero et al, 2013-a, Sosa et al, 2014-a); they included:

- Vertical gravity force is applied on the entire inflatable plug from the beginning to the end of the simulations.
- Air at ambient temperature of 80°F and standard ambient pressure is assumed to exist during the inflation of the plug.
- The volumetric values of air flow and inflation time are based on experimental results.

- Inflow air behaves as an ideal gas without heat transfer into the fluid cavity (adiabatic process).
- The air is assumed to be transferred into and within plug through an orifice which has a discharge coefficient of 1.0.
- The incoming air enters into the plug through the inflation fittings.
- The dynamic relaxation process applies to the model during entire deployment simulation.
- Internal chamber walls were used to direct the airflow inside the inflatable and to calculate the volume of fluid within the plug.
- The equivalent external fabric is assumed to be impermeable.

The model setup for simulation of deployment comprised the inclusion of a passive restraining mechanism consisting of multiple uniaxial ties installed in the surface of the inflatable during the folding process. The purpose of the ties is to produce a sequential release of membrane material in order to improve the level of local conformity on the walls and roof of the tunnel. These ties were represented by connector elements and are assumed to have translational degrees of freedom during the deployment simulation.

The model setup also included the creation of virtual internal chambers used to guide the airflow. The position of the internal chambers delimited by chamber walls placed inside the inflatable plug is illustrated in Figure 10. In this model, the inflation port is located in Chamber 2.

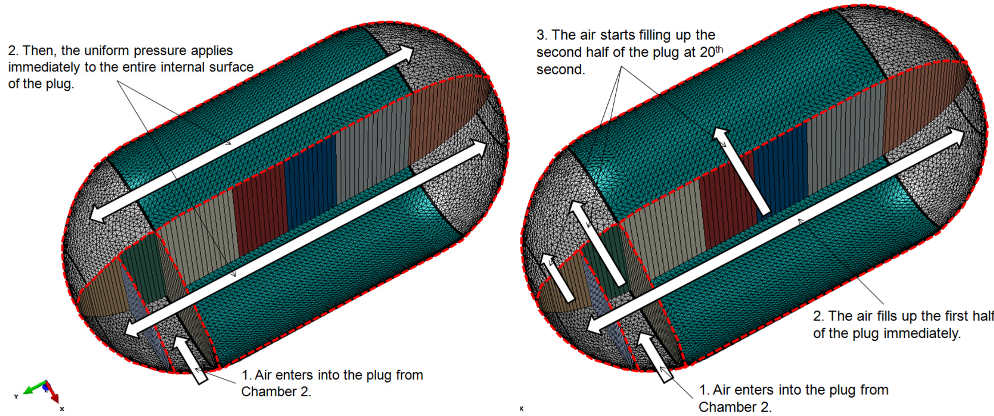


**(a)** **(b)**

**Figure 10: Position of chamber walls and flow direction within the inflatable plug; (a) Unguided airflow; (b) Guided airflow.**

## 5.2 Initial Configuration before Deployment

The folded plug placed in the storage area illustrated in Figure 9(d) was used as starting point of the deployment simulation. In this configuration, the folded plug sits on the base of the storage area under the effect of its own weight. A vertical virtual gate holds it up until the deployment sequence is activated. The folded plug is connected to the tunnel section at line B as shown in Figure 9(d), and the nodes of this line are fixed in all directions. This boundary condition represents the ties that fasten and restrain the inflatable plug to the tunnel section and are assumed to be unbreakable during the deployment simulation.

An unfolded reference configuration (initial metric) illustrated in Figure 10 was defined to specify the unfolded stress-free configuration of the inflatable plug. The folded plug illustrated in Figure 9(d) was used as initial configuration and the reference configuration were used to account for the wrinkles that arise from the folding process. Under this procedure, since a reference configuration was specified for all elements, any initial stress conditions specified for the same element are ignored, therefore no initial stresses were included in the membrane of the folded bag. Typically, during the modeling of folded membranes initial errors and mesh distortions are introduced inevitably during the folding process. This distortions in the folded mesh may lead to initial stresses that can affect the final shape of the deployed inflatable structure by creating fictitious wrinkles or bogus stress concentrations that do not exist in the real structure.

Gravity force and dynamic relaxation are applied on the folded plug from the very beginning of the simulation. Upon removal of the virtual vertical gate, the gravity force induces the fall of the plug, which starts to unroll and therefore initiating the deployment process. The tunnel section is assumed to be a rigid body fixed in X, Y, and Z direction. A friction coefficient 0.19 was used between plug and tunnel; and a self-friction coefficient of 0.21 was used for the fabric-to-fabric friction. These two values define how the surface of the membrane interacts with itself and the tunnel surface as the deployment develops in the simulation. The hard contact option was selected to be the contact method between parts.

The simulation plan showing various deployment conditions is summarized in Table 1. The folded plug in Deployment #1 did not include connector elements to control the release of membrane material; moreover, the air flow was not directed within the plug. When the air flow is not directed, the air fills up the plug evenly, spontaneously, and immediately once it enters into Chamber 2, as illustrated in Figure 10(a). The uniform pressure is calculated and applied on the entire internal surface of the plug when the airflow is not directed within the plug. Deployment #2 included connector elements installed during the folding process. For Deployment #3, a stiffness scale factor was included in the connector elements in order to compensate for the dynamic response associated to the mass scaling factor. Deployment #4 is similar to Deployment #3, but with a specific fluid exchange designed to guide the airflow within the plug. From Figure 10(b), the air fills up the first half (from Chamber 1 to Chamber 3) immediately after entering into the plug. After this initial step, the second half (Chamber 4) of the plug starts inflating at the 20$^{th}$ second.

**Table 1: Test Plan of Deployment Simulations.**

| Deployment # | Connector Elements | Air Flow Directed |
|---|---|---|
| 1 | No | No |
| 2 | Yes, without mass scaling | No |
| 3 | Yes, with mass scaling | No |
| 4 | Same as Deployment 3 | Yes |

## 5.3 Results

Figure 11 shows results corresponding to Deployments #1 and #4 as extreme cases compared to available experimental results. The airflow in Deployment #1, #2, and #3 was not directed, so the plug was inflated uniformly and instantaneously once the inflation part has been activated. The fluid exchange timing in Deployment #4 contributed to replicate the actual deployment performance.

The FE simulation can be used to evaluate the conformance, or fit, of the inflatable to the tunnel geometry. Lack of conformity reveals itself in the form of gaps between the inflatable and the tunnel wall, mainly observed at geometrical transitions such as corners and around obstructions such as pipes to which the inflatable has to adapt in order to seal. Lack of conformity is directly responsible for the leakage rate; that is, the flow rate that the plug is incapable of stopping, which obviously needs to be minimized. The simulation is also capable of predicting wrinkles in the plug fabric. The position and extension of wrinkles can be predicted accurately and they compare very well with experimental observations available in the literature. These wrinkles are the result of suboptimal deployment. Both wrinkles and gaps can be minimized by optimization of folding sequence; deployment sequence including air flow rate; position, number, and strength of passive restraining elements, and friction coefficient, among other factors. The effect on conformance of any and all of these factors, isolated or in combination, can be predicted by the simulation, thus minimizing the need for costly and time consuming experimentation. The excess of membrane material forms wrinkles on the tunnel wall instead of on the corner of the floor. This result is similar to what it was observed experimentally. The occurrence of wrinkles is in part related to how the membrane material is distributed and driven during the deployment, but it is also function of the percentage of manufacturing over sizing left in the perimeter of the cylindrical portion of the plug. The extra membrane material is added to account for unforeseen elements in the tunnel that can add to the perimeter to be sealed. It also accounts for the non-uniform nature of the deployment process that can lead to an irregular distribution of membrane material.

The level of global conformity of the plug to the tunnel section was evaluated by computing the contact area obtained for each deployment. Abaqus has the capability of computing the contact area between two objects, which in this case corresponded to the inflated plug and the tunnel walls. Table 2 summarizes the contact area for each deployment case. The cylindrical portion of the plug has a theoretical contact area of 71.98 $m^2$. This area should provide sufficient slippage resistance to handle an external force that will try to push the plug along the tunnel section that the plug itself is intending to seal.

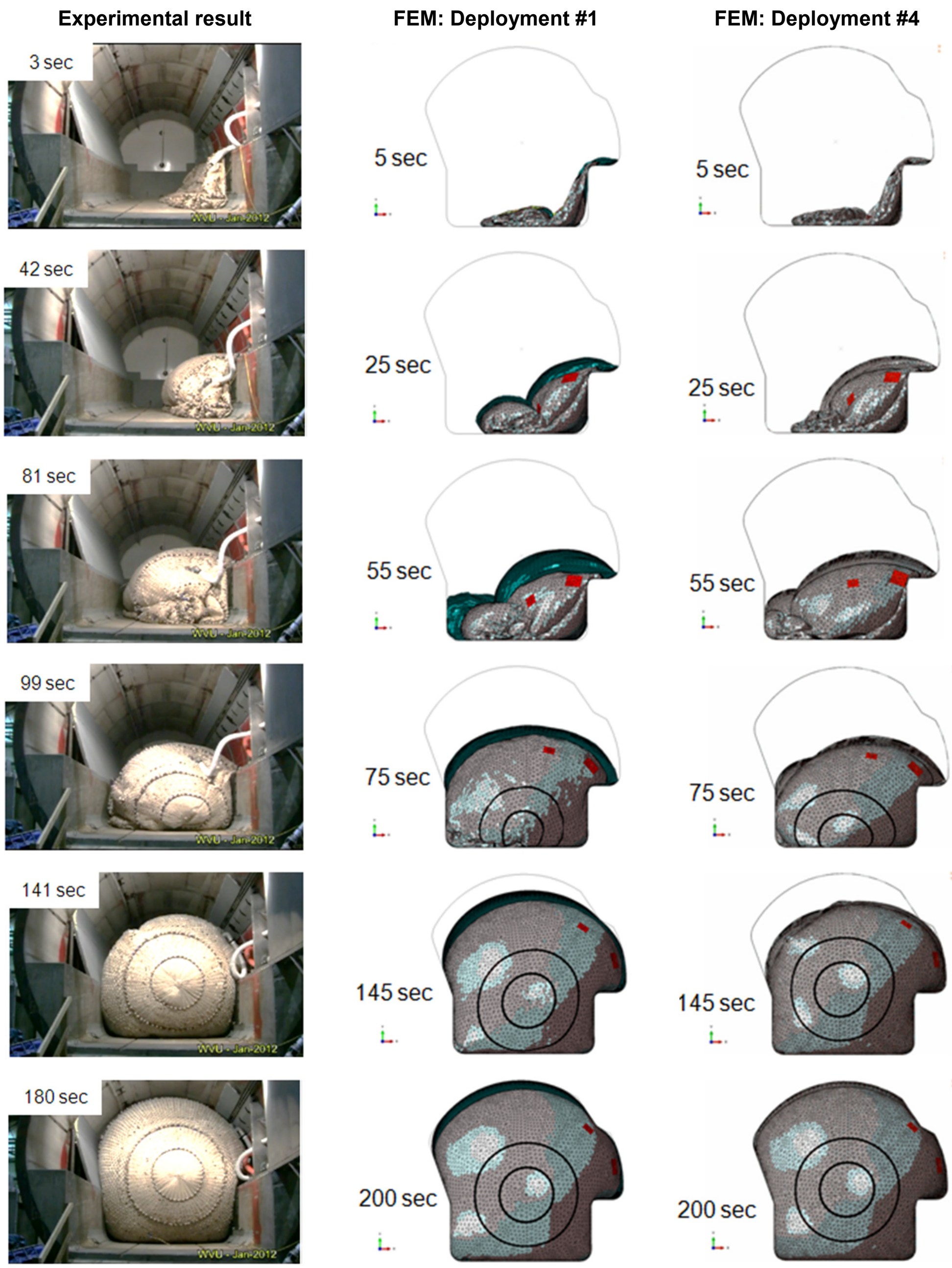


**Figure 11: Deployment sequences: Experimental (from Barbero et al, 2013-a, Sosa et al, 2014-a) vs. Deployments #1 and #4.**

Figure 12 shows a close-up view of experimental and simulation results illustrating the level of agreement reached by the finite element model particularly at the corners and change of angles in the perimeter of the tunnel.

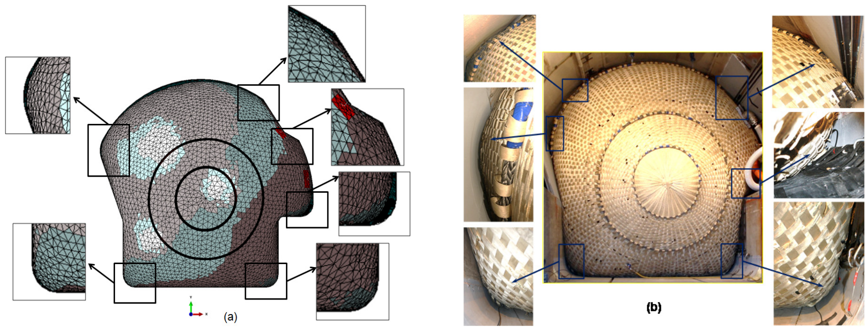


**Figure 12: Comparison of: (a) simulation results (Deployment #3) and (b) experimental results (Barbero et al, 2013-a, Sosa et al, 2014-a).**

Table 2 shows that for Deployment #1 the contact area increased 14% with respect to the original design contact area, even though the model did not include any connector elements to drive up membrane material, which created at least three bridging spots in the upper part of the tunnel, as observed in Figure 13. The extra contact area is generated by the confining effect of the tunnel section at the intersection of the hemispherical end-caps and the cylindrical part of the inflatable. The connector elements implemented in Deployment #2 failed earlier than expected. Still, the contact area increased 27% and reduced visible bridging to two places only. From the calculated contact area, the addition of connector elements clearly improves the global conformity by nearly duplicating the percentage of increase of contact area with respect to Deployment #1. Deployment #3 included connectors with scaled up elastic stiffness and failure force which delayed the breakage and left no visible bridging spots. Deployment #3 showed a contact enhancement of 32% with respect to the theoretical contact area. Deployment #4 predicted a contact enhancement slightly higher than Deployment #3 (+2%). Deployments #3 and #4 demonstrated to be the closest to the experimental results. The experimental contact area is not easily measurable, and it is not available for comparison with the simulation results. The simulation results demonstrate the advantage of using FE modeling to predict or estimate quantities, such as contact area, that cannot be obtained directly from physical experiments.

**Table 2: Contact Area after Completion of Deployment.**

| Parameter | Deployment # | | | |
|---|---|---|---|---|
| | 1 | 2 | 3 | 4 |
| Unconfined Inflation Cylindrical Contact Area (m²) | 71.98 | 71.98 | 71.98 | 71.98 |
| Confined Inflation Simulation Contact Area (m²) | 81.51 | 91.49 | 95.27 | 96.27 |
| Contact Enhancement % | +14% | +27% | +32% | +34% |
| Visible Bridging Spots | 3 | 2 | 0 | 0 |

## 6. Conclusions

This study presents the development of finite element models to simulate the installation and deployment of large confined inflatable structures. Models for folding, placement and deployment of an inflatable structure used to seal a closed conduct representative of a tunnel segment were presented. The strategy used for developing the models presented in this work can be used for further evaluations including design optimization of the inflatable, alternative folding sequences, and alternative ways to guide the air flow within the inflatable plug, as well as the influence of using different airflow rates during the deployment and inflation process. Alternative confining perimeters and additional features placed in the interior of the profile to maximize the sealing capacity of the plug can be modeled as well. The deployment simulation results as well as the level of conformity of the simulated inflatable structure to the confining perimeter are in excellent agreement with experimental results.

## 7. References


1. Abaqus User's Manual, Documentation Collection Version 6.11, Dassault Systémes Simulia Corp., Providence, RI.
2. Altair HyperWorks User's Manual. Altair Engineering Inc., Troy. MI.
3. Barbero, E. J., E. M. Sosa and G. J. Thompson. "Testing of Full-Scale Confined Inflatable for the Protection of Tunnels" Proceedings of the VI International Conference on Textile Composites and Inflatable Structures, Structural Membranes 2013, Munich, Germany, October 9-11, 2013 (a).
4. Barbero, E. J., E. M. Sosa, X. Martinez and J.M. Gutierrez, "Reliability Design Methodology for Confined High Pressure Inflatable Structures." Engineering Structures. Volume 51, pp. 1–9, June, 2013 (b).
5. Barrie A., "Going Underground: Homeland Security Works on Tool to Prevent Tunnel Disasters". FoxNews.com, September 05, 2008. http://www.foxnews.com/story/0,2933,417461,00.html
6. Fountain, H., "Holding Back Floodwaters with a Balloon", The New York Times/Science Supplement, Nov. 19, 2012. http://www.nytimes.com/2012/11/20/science/creating-a-balloonlike-plug-to-hold-back-floodwaters.html?pagewanted=all&_r=0
7. Martinez X., J. F. Davalos, E. J. Barbero, E. M. Sosa, W. Huebsch, K. Means, L. Banta, G. Thompson, "Inflatable Plug for Threat Mitigation in Transportation Tunnels". Proceedings of the Society for the Advancement of Material and Process Engineering Conference (SAMPE 2012), Baltimore, MD, May 21-24, 2012.
8. Peil K. L., E. J. Barbero, E. M. Sosa. "Experimental Evaluation of Shear Strength of Woven Webbings". Proceedings of the Society for the Advancement of Material and Process Engineering Conference (SAMPE 2012), May 21-24, Baltimore, MD, May 21-24, 2012.
9. Sosa, E. M., G. J. Thompson and E. J. Barbero, "Testing of Full-Scale Inflatable Plug for Flood Mitigation in Tunnels". Transportation Research Record: Journal of the Transportation Research Board, Volume 2407, Structures 2014, Vol. 2, pp. 59-67, 2014 (a).
10. Sosa, E. M., G. J. Thompson, E. J. Barbero, S. Ghosh, K. L. Peil. "Friction Characteristics of Confined Inflatable Structures", Friction, 2(4), pp. 365–390, November, 2014 (b).
11. Wang, J. T., and Nefske, O. J., "A new CAL3D Airbag Inflation Model," SAE paper 880654, 1988.